To be submitted to AFRC, Industrial Combustion Symposium October 2021

Experimental Investigation of Soot Formation in Inverse Co-Flow Flames at High Pressure

Ibrahim Alsheikh[1], Peng Liu[1], Abdulrahman Jamalallail[1], Raul Serrano Bayona[1], Sreenivasa Rao Gubba[1], Obulesu Chatakonda[2], Jeffrey W Kloosterman[3], William Roberts[1]

[1]Clean Combustion Research Center, King Abdullah University of Science and Technology (KAUST), Thuwal, 23955-6900, Saudi Arabia

[2]Air Products Technology Center, Dhahran Techno Valley, Dhahran, Saudi Arabia

[3]Air Products and Chemicals, Inc., Allentown, Pennsylvania, USA

Abstract

In this work, the effect of O_2 concentration on soot formation in inverse co-flow flames is comprehensively investigated. The fuel stream consists of a mixture of methane and CO_2, and the oxidant stream consists of O_2 and N_2. Diagnostic methods such as Laser-Induced Incandescence (LII) and Luminescence were employed. These techniques were used to probe soot volume fraction (SVF) and OH* intensity signals. Four sets of experiments were carried out at 4 bar to observe the effects of varied O_2 concentrations. In experiments, the O_2 concentrations were varied (70%, 58%, 46%, and 33% by volume) while the total oxidant stream was kept constant (i.e. 800 mL/min). Flowrates for both CH_4 and CO_2 were kept constant (1200 mL/min and 800 mL/min, respectively). Results reveal that soot loading in inverse co-flow flames decreases as O_2 concentration increases.

Key Words: *Inverse co-flow flame; Pressure; Soot; LII;*

1. Introduction:

The global shift from fossil fuels to clean and renewable energy is imminent. Hydrogen is a promising candidate to replace conventional sources of energy in the near future; due to its non-polluting nature [1]. Natural gas reforming has been proven to become a leading method for industrial hydrogen production, hydrogen is obtained from natural gas through a series of catalytic reactions [2]. Soot produced during the thermal reforming process does not only compromise the efficiency of catalysts used but it can deactivate the catalyst by depositing on the surface.

Therefore, increased attention can be noticed by researchers to understand the soot formation in such flames [3, 4].

Studying different flame operating parameters is essential to have a holistic understanding of soot formation. Oxygen concentration is largely important in combustion processes, as illustrated by oxy-fuel combustion. The effects of oxygen concentration in normal co-flow diffusion flames on soot formation at 1 bar have been investigated by Sun et al. [5], concluding that the increase in O_2 concentration would diminish soot formation. However, very few research studies were identified in the open literature on the oxygen concentration effects on soot formation in inverse co-flow flames at elevated pressures. An inverse co-flow flame at high pressure (where the central tube of the burner is the oxidizer and the outer tube is fuel) is chosen for our experimental setup since it has relevance in industrial applications due to its ability to combine features from both premixed and diffusion flames [6, 7]. Furthermore, the soot oxidation is excluded in inverse co-flow flame configuration, offering the opportunity to focus on soot formation and growth.

In this work, oxygen concentration effects on soot formation are thoroughly investigated in a methane inverse co-flow flame at elevated pressure (4 bar). Laser induced incandescence (LII) is used to measure SVF intensities, and chemiluminescence is utilized to obtain OH* signals.

2. Experiment Details:

2.1 Setup:

An inverse co-flow flame burner is placed inside an airtight vessel with a backpressure regulator to control the pressure inside the vessel. Gas feed pipes are installed on the bottom of the vessel flange. Inverse co-flow flame burner is made up of three concentric tubes each with a 1 mm thickness. Nitrogen is used to raise the pressure of the vessel and is flown symmetrically on either side of the burner. The oxidant stream is a mixture of N_2 and O_2 and is connected to the central tube of the burner with a 4 mm inner diameter (percentage of O_2 by volume is varied for different experiments). Whereas the fuel stream consists of CO_2 and CH_4 maintained at 800 and 1200 ml/min respectively, running through the first annulus with 10mm inner diameter. Lastly, through the second annulus with a 14mm inner diameter, a constant flow of 2 L/min of N_2 is used to minimize the buoyancy effects. Mass flow rate is controlled by calibrated Brooks thermal mass flow controllers (fluctuation < 2%). Figure 1 illustrates the experimental setup with other instruments employed such as Nikon CCD camera for flame images, ICCD camera to capture LII and OH* images, and a 1064 nm Nd: YAG laser. All these instruments are connected to a computer for data acquisition and LabVIEW is used for operation.

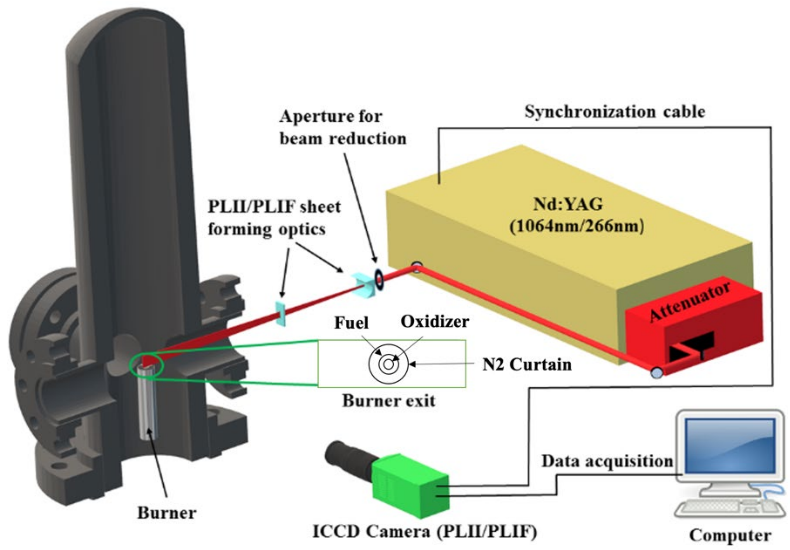

Figure 1. A high-pressure high-temperature experimental vessel with a burner in place along with a laser maneuvered through a series of lenses and mirrors.

2.2 Experimental conditions:

Four different oxygen concentrations i.e., 70%, 58%, 46%, and 33% by volume are chosen to understand the influence on soot nucleation, agglomeration, and production at a pressure of 4 bar. Test parameters and their respective volume flow rates are tabulated in Table 1.

Table 1. Parameters tested showing the different O_2 concentrations and volume flowrates.

Set	O_2, by Vol	Oxidant, mL/min	CO_2, mL/min	CH_4, mL/min	N_2 Curtain, L/min
1	70%	800	800	1200	2
2	58%	800	800	1200	2
3	46%	800	800	1200	2
4	33%	800	800	1200	2

3. Results and Discussion:

A Nikon CCD camera is used to capture images of the inverse co-flow flame at different O_2 levels. Images shown in Figure 2 indicate that with decreased O_2 concentrations, the flame becomes brighter due to higher soot loading. Furthermore, the inner blue flame height is almost not affected by changes in O_2 concentration.

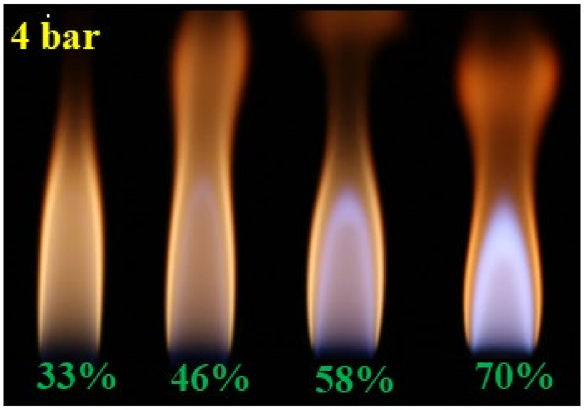

Figure 2. Images for flames with different O_2 concentrations in oxidizer steam.

3.1 OH* Images:

OH* signal information is captured using an ICCD camera and narrowband filter (310±10 nm), as shown in Figure 3. It is evident from both Figures 2 and 3 that flame height is unchanged with an increase in O_2 concentration. Furthermore, with an increase in oxygen levels, OH* signal intensity increases, and the peak concentration of OH* is always located on the flame tip.

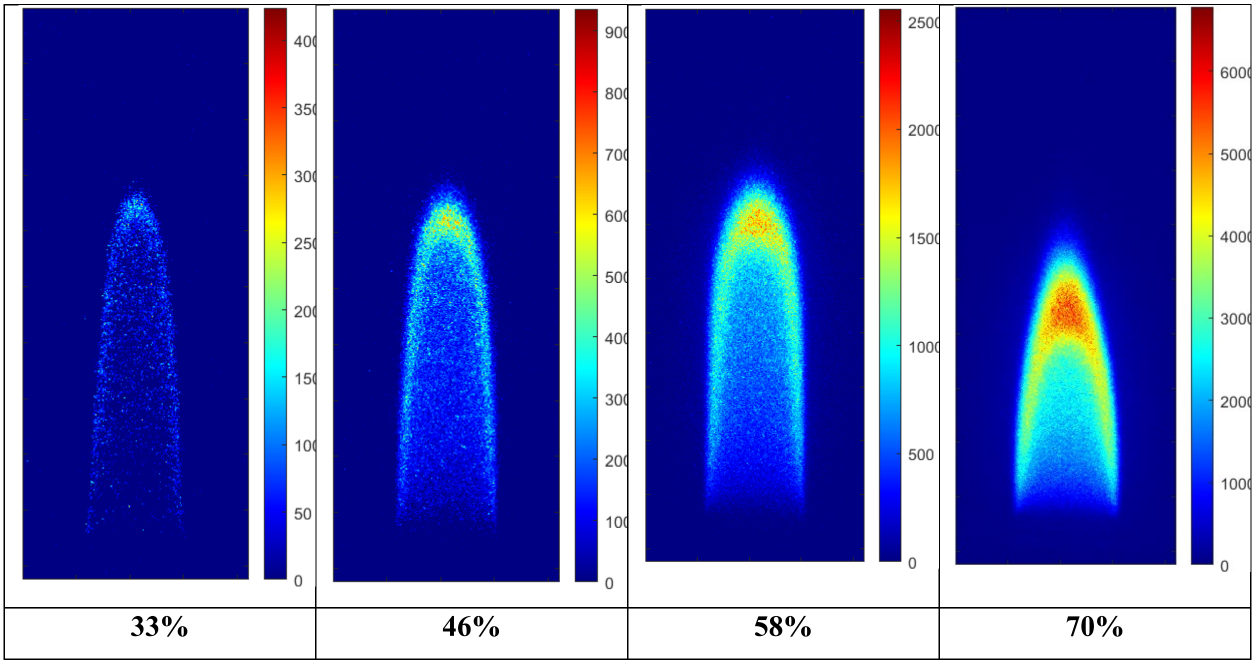

Figure 3. OH* intensity signal at 4 bar, illustrating the effect of O2 concentration on the flame structure. The individual color legend is presented for each image.

3.2 LII Images:

LII diagnostics allow us to capture the soot distribution of the inverse co-flow flame. Figure 4 shows the effects of oxygen concentrations on soot formation at 4 bar. It is evident that with increasing oxygen levels soot is forming closer to the burner nozzle. When the O_2 concentration is lower, the soot formation structure on either side of the flame is found to have a smaller gap. Also, experimental data from the individual legend in Figure 4 suggests that soot formation is greatly sensitive to O_2 concentration.

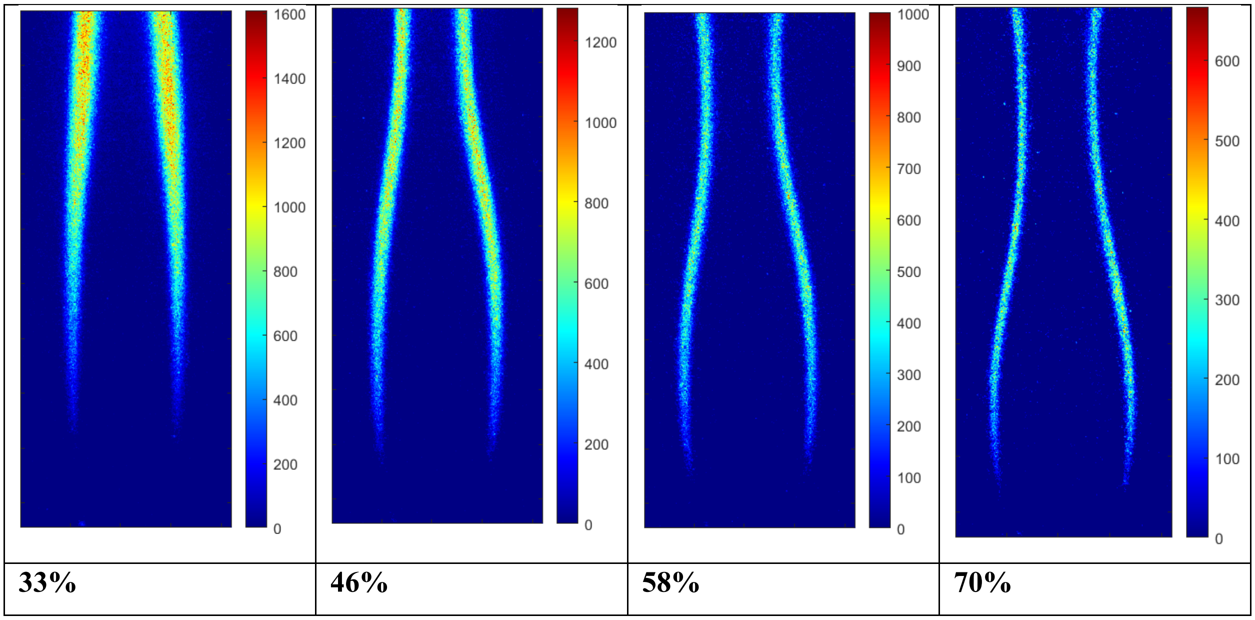

Figure 4. Raw LII images for flames with different O_2 concentrations in oxidizer steam at 4 bar. Laser crosses the flame from the right to the left side (Individual color legend is presented for each image).

3.3 Quantitative results:

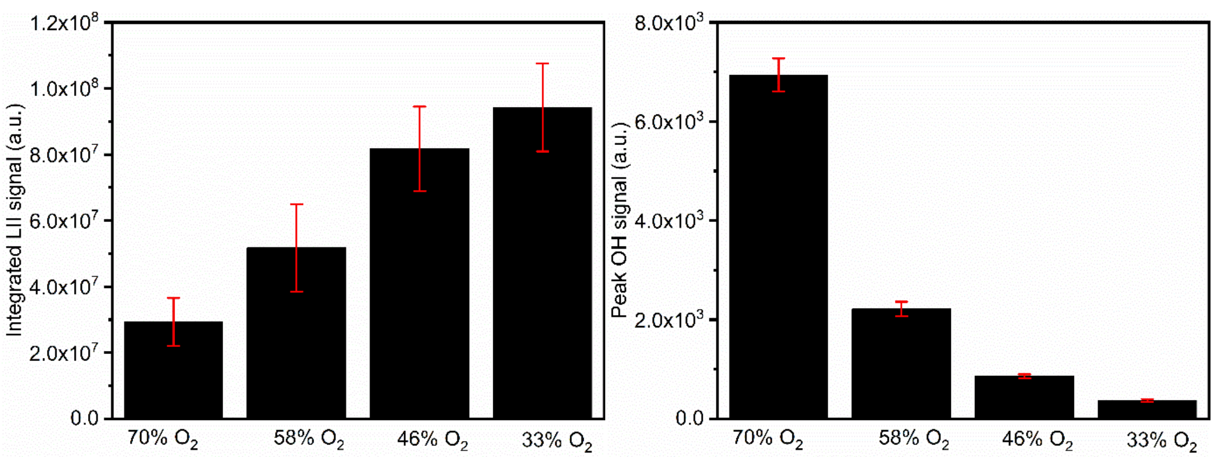

Figure 6. (a) Integrated LII intensity vs O_2 concentration at 4 bar. (b) Peak OH* intensity vs O_2 concentration at 4 bar.

The integrated LII is obtained by taking the sum of all signals. The red error bar shows the standard deviation from the 300 images captured. As shown in Figure 6(a), the integrated LII signal intensity is higher for the flame with lower oxygen levels. In the investigated flame configuration, soot oxidation is minimized, so the soot loading is dominantly controlled by soot growth.

Numerous evidence indicates that soot growth is mainly determined by the concentration of soot precursor PAH, flame temperature, the concentration of relevant gas-phase small hydrocarbon species [8-10]. OH* could be an indicator of flame temperature. The peak flame temperature is seen with a higher O_2 level, as evidenced by the trend of the peak signal intensity of OH* in Figure 6(b). Measurements regarding PAH and small hydrocarbon species should be conducted in the future, for a better understanding of soot enhancement by lowering the O_2 concentration.

Conclusion:

Effects of O_2 concentration at elevated pressure in methane Inverse Co-flow flames were investigated comprehensively. Laser induced incadenscence was used to capture the soot profile and intensity while OH* distribution was captured using chemiluminescence. Conclusions made were:

- The flame height is stable across varying O_2 levels, OH* peak values increase with decreasing O_2 concentration. Visually we see that OH* is concentrated on the flame tip.
- O_2 Concentration effects on soot formation in inverse co-flow flames are substantial. A higher O_2 in oxidant steam is needed to lower SVF intensity. Visually using LII images we see that soot forming on the wings of the flame has a narrower gap in between them and farther away from the burner nozzle with decreased O_2 levels.

Acknowledgments:

The research reported in this paper was supported through funding from King Abdullah University of Science and Technology (KAUST), the Clean Combustion Research Center (CCRC), and Air Products through its projects of RGC/3/4490-01-01.

References:

1. Paolo Zeppini, Jeroen C.J.M. van den Bergh, Global competition dynamics of fossil fuels and renewable energy under climate policies and peak oil: A behavioural model, Energy Policy, Volume 136, 2020, 110907, ISSN 0301-4215, https://doi.org/10.1016/j.enpol.2019.110907.

2. M.H. Halabi, M.H.J.M. de Croon, J. van der Schaaf, P.D. Cobden, J.C. Schouten, Modeling and analysis of autothermal reforming of methane to hydrogen in a fixed bed reformer, Chemical Engineering Journal, Volume 137, Issue 3, 2008, Pages 568-578, ISSN 1385-8947, https://doi.org/10.1016/j.cej.2007.05.019.

3. Qing He, Qinghua Guo, Kentaro Umeki, Lu Ding, Fuchen Wang, Guangsuo Yu, Soot formation during biomass gasification: A critical review, Renewable and Sustainable Energy Reviews, Volume 139, 2021, 110710, ISSN 1364-0321, https://doi.org/10.1016/j.rser.2021.110710.

4. Yeidy Sorani Montenegro Camacho, Samir Bensaid, Souzana Lorentzou, Nunzio Russo, Debora Fino, Structured catalytic reactor for soot abatement in a reducing atmosphere, Fuel Processing Technology, Volume 167, 2017, Pages 462-473, ISSN 0378-3820, https://doi.org/10.1016/j.fuproc.2017.07.031.

5. Zhiwei Sun, Bassam Dally, Zeyad Alwahabi, Graham Nathan, The effect of oxygen concentration in the co-flow of laminar ethylene diffusion flames, Combustion and Flame, Volume 211, 2020, Pages 96- 111, ISSN 0010-2180, https://doi.org/10.1016/j.combustflame.2019.09.023.
6. Rodrigo Demarco, Alejandro Jerez, Fengshan Liu, Longfei Chen, Andrés Fuentes, Modeling soot formation in laminar coflow ethylene inverse diffusion flames, Combustion and Flame, Volume 232, 2021, 111513, ISSN 0010-2180, https://doi.org/10.1016/j.combustflame.2021.111513.

7. Filipe M. Quintino, Miguel Ribeiro, Edgar C. Fernandes, Structure of CH4–Air Inverse Diffusion Flames in a Multi-slit Burner, Energy Fuels 2021, 35, 9, 7217–7231, https://doi.org/10.1021/acs.energyfuels.0c03830

8. Peng Liu, Zepeng Li, Anthony Bennett, He Lin, S Mani Sarathy, William L Roberts, The site effect on PAHs formation in HACA-based mass growth process. Combustion and Flame, 199, 54-68. https://www.sciencedirect.com/science/article/pii/S0010218018304371

9. Anthony M Bennett, Peng Liu, Zepeng Li, Najeh M Kharbatia, Wesley Boyette, Assaad R Masri, William L Roberts, Soot formation in laminar flames of ethylene/ammonia, Combustion and flame, 2020, 220, 210-218. https://www.sciencedirect.com/science/article/pii/S0010218020302601

10. Peng Liu, Zepeng Li, William L Roberts, The growth of PAHs and soot in the post-flame region. Proceedings of the Combustion Institute, 37, 977-984. https://www.sciencedirect.com/science/article/pii/S1540748918300488